*Oncology Research*, Vol. 25, pp. 295–304
Printed in the USA. 

0965-0407/17 $90.00 + .00
DOI: https://doi.org/10.3727/096504016X14732527645922
E-ISSN 1555-3906
www.cognizantcommunication.com



# Intratumoral Photodynamic Therapy With Newly Synthesized Pheophorbide a in Murine Oral Cancer

Mee-Young Ahn,*[1] Hyo-Eun Yoon,†[1] Seong-Yong Moon,‡ Yong-Chul Kim,§ and Jung-Hoon Yoon†

*College of Medical and Life Sciences, Division of Bio-industry, Major in Pharmaceutical Engineering, Silla University, Busan, South Korea
†Department of Oral and Maxillofacial Pathology, College of Dentistry, Wonkwang Bone Regeneration Research Institute, Daejeon Dental Hospital, Wonkwang University, Daejeon, South Korea
‡Department of Oral and Maxillofacial Surgery, School of Dentistry, Chosun University, Gwangju, South Korea
§Department of Life Sciences, Gwangju Institute of Science and Technology, Gwangju, South Korea

Photodynamic therapy (PDT) is a therapeutic alternative for malignant tumors that uses a photosensitizer. Our group recently synthesized photosensitizer pheophorbide a (Pa) from chlorophyll-a. The present study investigated the therapeutic effect of PDT using intratumoral administration of the synthetic photosensitizer Pa in an in vivo murine oral squamous cell carcinoma (OSCC) animal model. Pa accumulation was measured using the fluorescence spectrum and imaging in living C3H mice. Intratumoral treatment of Pa-PDT (IT Pa-PDT) significantly inhibited the growth of transplanted OSCC cells. Histopathological examination of tumor tissues showed that PCNA expression was significantly decreased, while TUNEL-stained cells were markedly increased in the IT Pa-PDT group compared to controls. IT Pa-PDT-induced apoptosis was confirmed by immunoblot. Reduction of Bcl-2 and cleavage of caspase 3 and PARP were observed in IT Pa-PDT. These data demonstrate that IT Pa-PDT inhibited tumor cell proliferation and induced apoptosis, which is correlated with the anticancer activity of IT Pa-PDT. These potent antitumor activities of IT Pa-PDT were observed in both the immunohistochemistry and Western blot experiments. Our findings suggest the intratumoral therapeutic potential of Pa-PDT on OSCC. Additionally, demonstrated detection of Pa using a fluorescence spectroscopy system or molecular imaging system provides a means for simultaneous diagnosis and treatment of OSCC.

**Key words: Pheophorbide a (Pa); Photodynamic therapy (PDT); Intratumoral administration; Oral squamous cell carcinoma (OSCC)**

## INTRODUCTION

Photodynamic therapy (PDT) is a nonsurgical alternative for the treatment of several diseases, including cancer. PDT offers the potential efficacy of tumor clearance with good cosmesis, patient tolerability, and brief healing time compared with conventional surgery[1]. PDT involves the use of photochemical reactions mediated through the interaction of photosensitizing agents, light, and oxygen. The photosensitizer is activated by receiving light energy to produce singlet oxygen and other reactive oxygen species, which causes oxidative stress in cells and membrane damage and finally leads to cell death and tumor destruction[2–5]. More than 400 compounds with photosensitizing properties are known including dyes, drugs, cosmetics, chemicals, and natural substances[6]. Limited photosensitizers have been used for clinical PDT, and second-generation photosensitizers are also undergoing clinical evaluation[7]. Among them, pheophorbide a (Pa) is a chlorine-based second-generation photosensitizer that is derived from chlorophyll-a with photo-dependent or -independent cytotoxic activity[8,9]. Pa was identified as an active antitumor component from a number of traditional medicine sources such as *Scutellaria barbata*, *Psychotria acuminata*, and silkworm excretan[10,11]. Previous studies have suggested the therapeutic efficacy of Pa-mediated PDT, which was investigated in leukemia, hepatocellular carcinoma, colon cancer, and pigmented melanoma[10,11]. Recently, our group synthesized Pa by removing a magnesium ion and a phytyl group from chlorophyll-a, which may be more easily available for commercial use than

[1]These authors provided equal contribution to this work.
Address correspondence to Jung-Hoon Yoon, D.D.S., Ph.D., Department of Oral and Maxillofacial Pathology, College of Dentistry, Daejeon Dental Hospital, Wonkwang University, Daejeon 302-120, South Korea. Tel: 82-42-366-1146; Fax: 82-42-366-1115; E-mail: opathyoon@wku.ac.kr

purified Pa from plants[12,13] (Fig. 1). We then evaluated the antitumor effect of PDT with synthesized Pa on human oral squamous cell carcinoma cells in vitro[13].

The response to PDT may vary not only with the cell type or its metabolic potential but also with total fluence delivered, different types of photosensitizers, and their intracellular localization[14]. A photosensitizer is one of the principal components for an effective photodynamic process and typically administered to the patient by intravenous (IV) injection[15]. The photosensitizing drug is especially absorbed by the cancer cells while sparing much of the nearby healthy cells, and the treatment area is exposed to a spectrum of light, which activates the drug to destroy cancer cells. However, the poor cancer cell uptake and inefficient tumor delivery of photosensitizing agents limit the current applications of PDT in cancer therapy[16]. In order to improve the performance of photosensitizers, they should be targeted specifically to the tumor cells. Theoretically, high sensitizer concentrations in tumor tissue can be obtained by direct application of the photosensitizer into the tumor[17].

In this study, we examined the therapeutic effect of PDT with intratumorally injected synthesized Pa (IT Pa-PDT) on suppressing tumor growth in an in vivo murine oral cancer model. C3H mice bearing AT-84 murine oral cancer cells were treated with IT Pa-PDT, and its effect on tumor growth was monitored. The effect of IT Pa-PDT on inducing apoptosis was also analyzed in vivo.

## MATERIALS AND METHODS

### *Cell Culture*

AT-84 cells, murine OSCC cell lines, were provided by Dr. E. J. Shillitoe (State University of New York, Upstate Medical University) and have been described previously[18]. The cells were maintained in RPMI-1640 medium (Invitrogen, Eugene, OR, USA) containing 10% fetal bovine serum (Invitrogen) and 1% penicillin–streptomycin (Welgene, Daegu, South Korea) and subsequently incubated at 37°C in an atmosphere containing 5% $CO_2$.

### *Preparation of Pa*

Pa was synthesized according to the procedure described previously[12]. Briefly, treatment of the ethanol solution of chlorophyll-a in an acidic condition (1 N HCl, pH 2.5) easily enabled the removal of the $Mg^{2+}$ ion to afford a crude pheophytin in the form of precipitates. The pheophytin was subsequently hydrolyzed by reacting with 80% trifluoroacetic acid (TFA) in water to make Pa a fine powder.

### *Cellular Uptake in AT-84 Cells*

Cells were seeded in a 60-mm dish and incubated for 24 h to allow attachment. After washing with PBS, the cells were incubated with 0.25 μM Pa for the indicated time periods in serum-free culture medium. Cells were washed with PBS and changed to fresh media. The cellular uptake of Pa (red signal, 655- to 755-nm emission) was examined up to 24 h using Olympus IX71 fluorescence microscopy (Tokyo, Japan).

### *Photodynamic Treatment*

AT-84 cells were incubated in a serum-free culture medium with Pa for 2 h. After washing, the cells were exposed to a light dose of 4.24 J/cm$^2$, performed using a laser diode (Geumgwang Co. Ltd., Daejeon, South Korea) at a wavelength of 664 nm.

### *MTT Assay*

Cells ($2\times10^4$ cells/well) were seeded in a 24-well plate and incubated for 24 h to allow attachment. After washing with PBS, the cells were incubated with Pa for 2 h followed by irradiation. After 24 h, the cells were washed

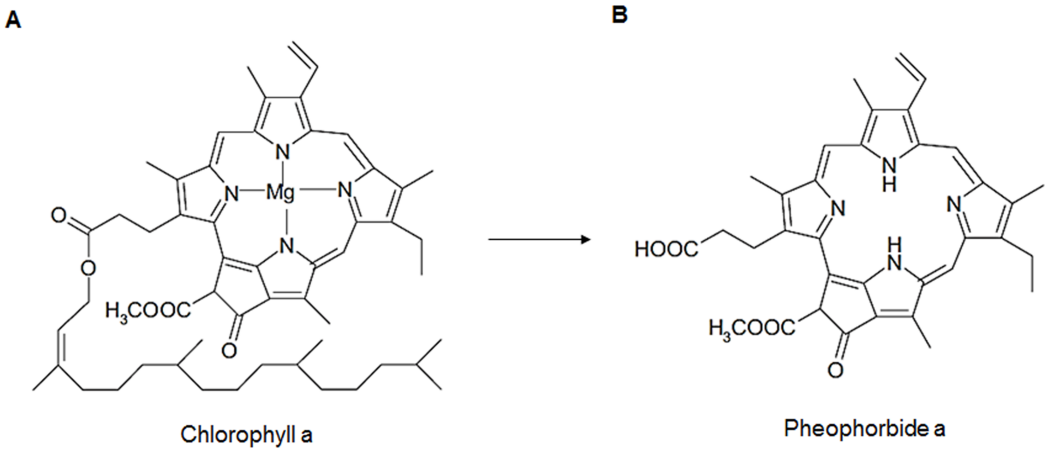


**Figure 1.** Chemical structures of chlorophyll-a (A) and synthesized pheophorbide a (B).

twice with PBS, and 0.5 ml of cell culture medium and 50 µl of 3-(4,5-dimethylthiazol-2-yl)-3-5-diphenyltetrazolium bromide solution (5 mg/ml) (Sigma-Aldrich, St. Louis, MO, USA) were added. After 3 h of incubation, medium was removed, and 250 µl of dimethyl sulfoxide (DMSO) was added. The absorbance was measured at 595 nm by the Microplate Autoreader ELISA (Beckman Coulter, Wals-Siezenheim, Austria), and all experiments were performed in triplicate.

*Fluorescence Spectroscopy Mode*

One week after inoculation of AT-84 cells, the mice were administered an intratumoral injection with photosensitizer Pa at a dosage of 10 mg/kg. Fluorescence spectra of the tumor regions of the skin of the mice were monitored after the photosensitizer injection. The fluorescence spectrum from Pa was measured using the fluorescence spectroscopy (FS) system according to the procedure described previously[19]. Sensitizers have an emission peak near 675 nm under excitation at 405 nm.

*Imaging*

C3H mice were imaged with the Xenogen IVIS Imaging System (Xenogen Co., Alameda, CA, USA) to record the bioluminescent signal emitted from the tumor. The IVIS-100 was equipped with a CCD camera system, which was used for emitted light acquisition, and the Living Image software (Xenogen) was used for data analysis.

*In Vivo Study of IT Pa-PDT on AT-84 Cell-Bearing CH3 Mice*

AT-84 cells were used for in vivo experiments, which was previously established by Pang et al.[20]. Six-week-old male immunocompetent C3H mice (Samtaco, Sungnam, South Korea) were inoculated subcutaneously on the right flank with $1\times10^7$ AT-84 cells. One week later, the animals were administered intratumorally at a dosage of 10 mg/kg Pa. After 2 h, PDT was performed using a laser diode at a light dose of 100 J/cm$^2$ and wavelength of 664 nm. The animals were monitored daily, and tumor volume was measured by caliper and calculated by the formula: $V=(ab^2)/2$, in which $a$ is the longest diameter, and $b$ is the shortest diameter of the tumor. All experiments were performed under protocols approved by the Animal Care and Use Committee at Wonkwang University, Department of Dentistry.

*Histopathology, Immunohistochemistry, and TUNEL Assay*

The animals were euthanized on day 15, and the tumors were removed carefully and fixed in 10% formalin over 24 h. The tissues were then dehydrated in an alcohol–xylene series and embedded in paraffin wax. From each block, 2-µm-thick sections were prepared and stained with hematoxylin (Vector, Burlingame, CA, USA) and eosin (H&E) for histological examination. For immunohistochemistry, the sections were incubated in 3% $H_2O_2$ in methanol for 10 min to remove endogenous peroxidase and blocked with 1% BSA in PBS for 1 h. The sections were then incubated with PCNA antibody (Dako, Carpinteria, CA, USA) overnight at 4°C. After washing three times with PBS-T, the sections were subjected to the avidin–biotin peroxidase complex (ABC) method (Vector), and peroxidase activity was evaluated with 3,3′-diaminobenzidine (Vector). Finally, the sections were counterstained with hematoxylin. The terminal deoxynucleotidyl transferase-mediated dUTP nick-end labeling (TUNEL) assay was done using an Apoptosis Detection Kit (Millipore, Billerica, MA, USA) according to the manufacturer's protocol. PCNA-positive cells and apoptotic cells were counted from five randomly selected areas under 200× magnification and represented as mean ± SD.

*Western Blot Analysis*

The animal tissues were homogenized in a lysis buffer containing 50 mM Tris-HCl (pH 7.5), 150 mM NaCl, 1 mM EDTA, 2.5 mM EGTA, 10% glycerol, 1 mM dithiothreitol, 100 mM phenylmethyl sulfonyl fluoride, 10 µg/ml aprotinin, and 10 µg/ml leupeptin. The protein concentrations were quantified using a Bio-Rad protein assay reagent (Bio-Rad Laboratories, Hercules, CA, USA) according to the manufacturer's protocol. The total protein (50 µg per lane) was resolved by 7.5%–15% SDS-PAGE and transferred onto polyvinylidene difluoride (PVDF) membrane (NEN Life Science, Boston, MA, USA). After blocking in TBS (20 mmol/L Tris, 137 mmol/L NaCl, 1 g/L Tween 20, pH 7.6) with 5% skim milk for 1 h at room temperature, the membranes were incubated with primary antibodies against cleaved caspase 3, PARP (Cell Signaling, Beverly, MA, USA), PCNA (Abcam, Cambridge, MA, USA), Bcl-2, and actin (Santa Cruz Biotechnology, Santa Cruz, CA, USA) overnight at 4°C. The membranes were then washed three times with TBS-T and incubated with secondary antibodies (Santa Cruz Biotechnology) for 1 h at room temperature. Finally, the membranes were washed three times with TBS-T and visualized using the ECL detection reagent (Millipore) on the LAS-1000 image system (Fujifilm, Japan).

*Statistical Analysis*

All statistical analyses were carried out using Excel software. Data are expressed as the mean ± SD of at least three individual experiments. Statistical comparisons between groups were performed using two-tailed Student's $t$-test. Statistical significance was set at $p<0.05$, $p<0.01$, and $p<0.001$.

## RESULTS

### *Photosensitizer Pa Accumulation in AT-84 Cells*

The cellular uptake of Pa in AT-84 cells was examined 30 min and up to 24 h after treatment with 0.25 μM Pa using fluorescence microscopy. As shown in Figure 2A, accumulation of Pa in AT-84 cells was markedly observed 2 h after incubation with 0.25 μM Pa. Pa red fluorescence was continually observed in the cells up to 24 h after incubation, but no fluorescence signal was observed in the control group. From these results, Pa administration for 2 h after treatment was selected for the following experiments.

### *The Effect of Pa-PDT on the Inhibition of Cellular Proliferation in AT-84 Cells*

To investigate whether Pa-PDT inhibits cell proliferation of AT-84 cells, the cells were treated with various doses of Pa for 24 h. The results of the MTT assay revealed that Pa-PDT significantly inhibited proliferation of AT-84 cells in a dose-dependent manner with up to 1 μM Pa treatment (Fig. 2B). However, there was no cytotoxicity in cells treated with Pa or laser alone. The $IC_{50}$ value for Pa-PDT was 0.25 μM.

### *In Vivo Monitoring of Pa Accumulation After Intratumoral Injection*

Pa was intratumorally administered to mice inoculated with AT-84 cells. We next measured the fluorescence spectra of the tumor tissues of mice injected with Pa (10 mg/kg). The fluorescence signal was clearly observed in Pa-injected tumor tissues, but not in the control tissues (Fig. 3A and B). The main fluorescence peak of Pa was also observed at ~672 nm, indicating that the Pa had successfully accumulated in the tumor tissues. For the purpose of analyzing the fluorescence of Pa in living C3H mice, we also confirmed fluorescence imaging up to 6 h using the IVIS Imaging System. As shown in Figure 3C, strong fluorescence imaging could be obtained in mice intratumorally injected with Pa until 6 h, whereas the red fluorescence signal was not observed in control mice. From these results, Pa administration for 2 h of treatment was selected for in vivo experiments.

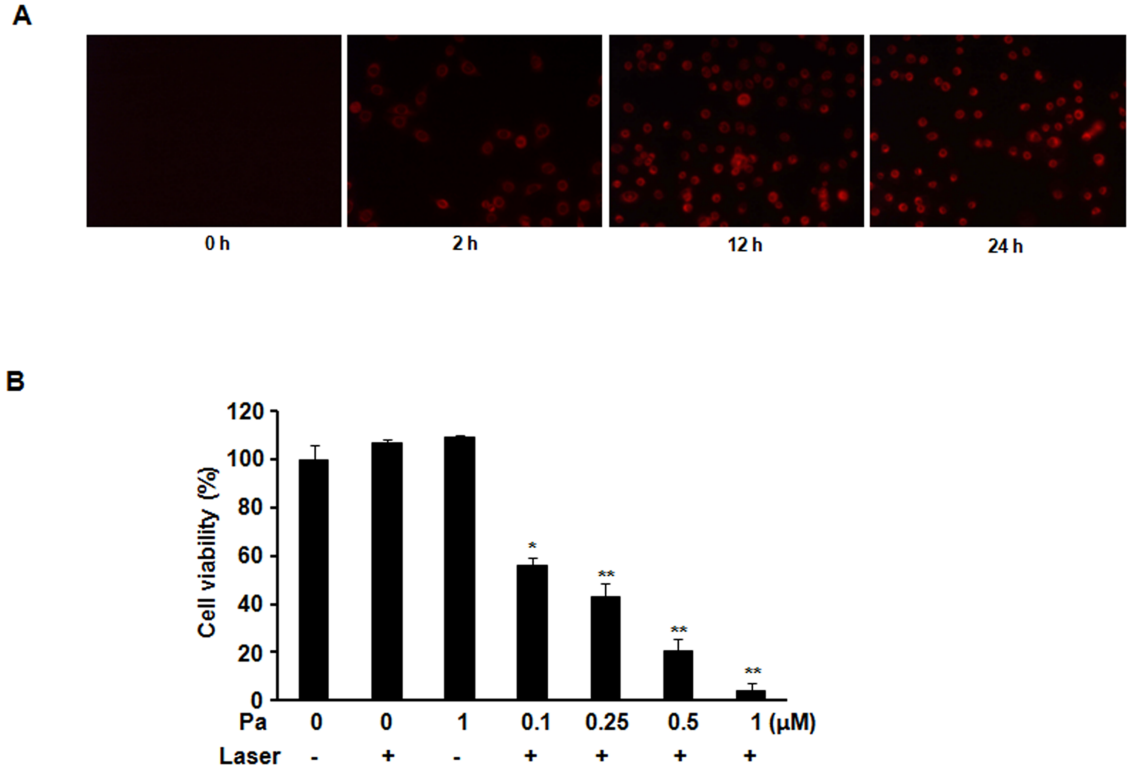


**Figure 2.** Pa accumulation and growth inhibition by Pa-PDT in AT-84 cells. (A) The cells were incubated with 0.25 μM Pa for up to 24 h, and photographs were obtained by fluorescence microscopy (magnification: 200×). (B) The cells were incubated with the indicated concentrations of Pa for 2 h followed by exposure to 4.24 J/cm$^2$ of laser light for 24 h. The levels of cell proliferation were measured using an MTT assay. The percentage of viable cells was calculated as the ratio of treated cells to control cells. The data are reported as the mean ± SD of three independent experiments. *$p < 0.05$, **$p < 0.01$ compared to untreated control.

*The Inhibition Effect of IT Pa-PDT In Vivo Tumor Growth*

The in vivo effect of IT Pa-PDT on tumor growth was examined using mice inoculated with AT-84 cells. After Pa accumulation for 2 h, PDT was performed using a laser diode, and tumor volume was measured every other day after IT Pa-PDT. As shown in Figure 4A and B, IT Pa-PDT significantly decreased tumor volume compared to the control group and inhibited tumor growth up to 60% relative to the control group at the end of periods. The durability of Pa administration in the Pa-PDT-treated tumor tissues was also examined using fluorescence imaging system in the mice during the experimental periods. As shown in Figure 4C, the strong red fluorescence signal was continuously observed in IT Pa-PDT-treated mice until 14 days. However, no systemic toxicity, including body weight changes and other apparent adverse effects, was observed in the animals throughout the study period (Fig. 4D). These results showed that IT Pa-PDT effectively inhibits tumor growth.

*Immunohistochemical Expression of PCNA and TUNEL Assay*

Histopathological evaluation was examined in paraffin-embedded tumor sections using H&E staining. Solid growth of SCC with mitotic figures and hemorrhage was observed in control tumor tissues, whereas extensive cell death with some necrosis with nuclear pyknosis and cytoplasmic eosinophilia was observed in IT Pa-PDT-treated tumor tissues (Fig. 5A, top). The antitumor effects of IT Pa-PDT were next performed by examining the immunohistochemistry of PCNA, a cell proliferation marker, and TUNEL staining for assessing the amount of apoptotic cells in paraffin-embedded tumor sections. The percentage of cancer cells with a positively stained nucleus for PCNA was markedly decreased in the IT Pa-PDT-treated

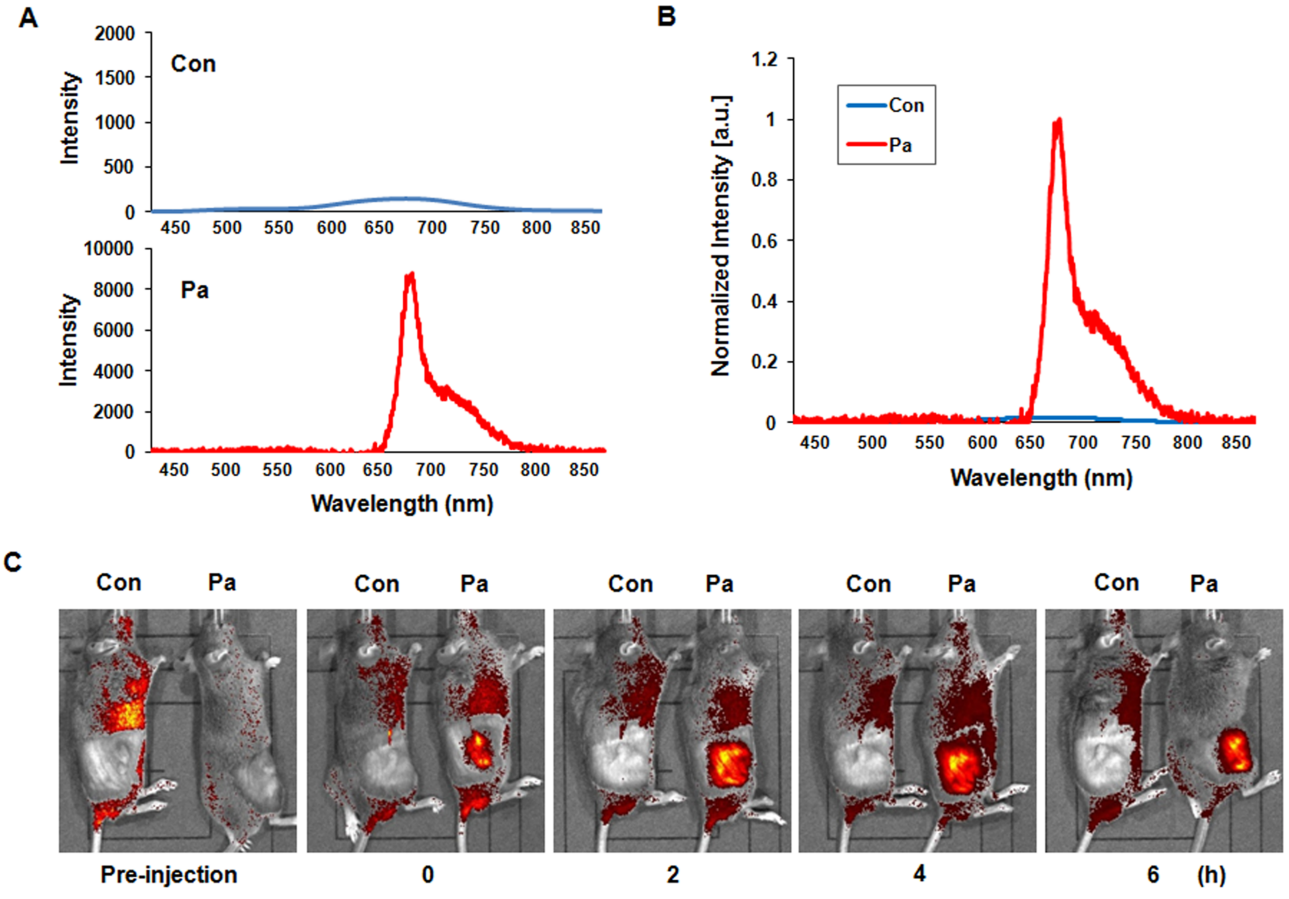


**Figure 3.** Pa accumulation in the in vivo C3H mice model. Photosensitizer Pa (10 mg/kg) was injected intratumorally into the right flank of C3H mice. (A) The fluorescence spectra were measured from tumor tissues of the control and Pa-treated groups, respectively, using the fluorescence spectroscopy (FS) system. (B) The peak intensity was compared between the control and Pa-treated group. The main fluorescence peaks were observed at ~672 nm in Pa-treated tumor tissues. (C) In vivo fluorescence imaging was obtained using the Xenogen IVIS-100 Imaging System equipped with a CCD camera system.

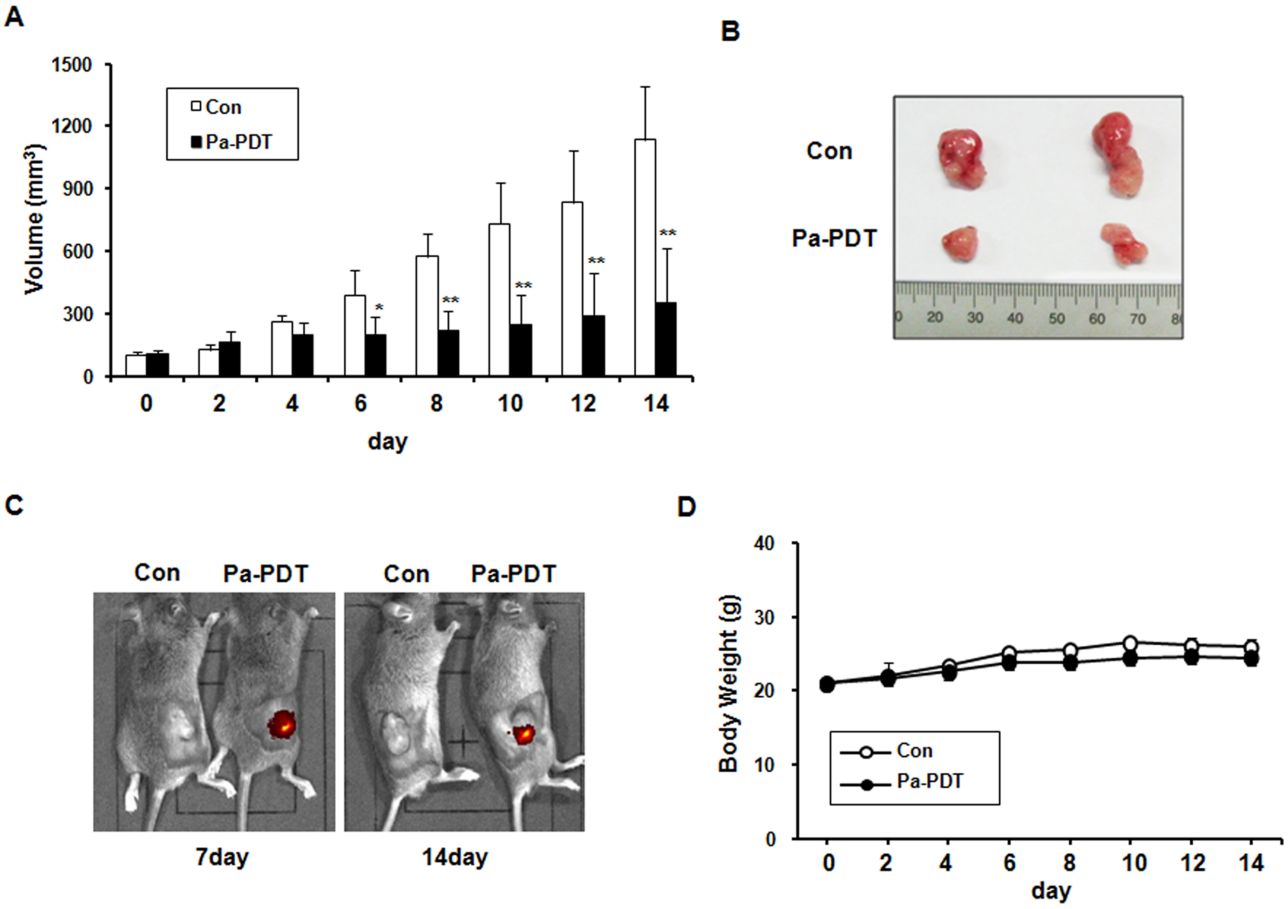


**Figure 4.** Effect of IT Pa-PDT on tumor growth in an in vivo model. (A) Relative tumor volumes in mice inoculated with AT-84 cancer cells. Relative tumor volumes of the mice treated with IT Pa-PDT and the vehicle-treated controls. The tumor volumes were measured and transformed subsequently to the relative tumor volume, as detailed in Materials and Methods. The data are reported as the mean ± SD of five animals. $*p<0.05$, $**p<0.01$ as determined by a Student's *t*-test compared to the control group. (B) In situ appearance of tumors in the control and Pa-PDT-treated mice. (C) In vivo fluorescence imaging of Pa was obtained using the Xenogen IVIS-100 Imaging System equipped with a CCD camera system. (D) An assessment of body weight between the Pa-PDT-treated and control mice during the entire experimental period. The body weight of mice in different groups was recorded every alternate day.

group compared to the control group with $p<0.01$ [Fig. 5A (middle) and B (top)]. IT Pa-PDT treatment significantly increased the TUNEL-positive apoptotic cell population, compared to those in the control group with $p<0.001$ [Fig. 5A (bottom) and B (bottom)]. These results showed that the induction of apoptosis by the IT Pa-PDT treatment may be associated with the anticancer activity of IT Pa-PDT in vivo.

### *The Expression of Apoptosis-Related Proteins in Tumor Tissues*

To determine the apoptotic mechanism of IT Pa-PDT in vivo, the expression levels of apoptosis-related proteins were monitored by Western blot analysis with tumor homogenates. As shown in Figure 6, the levels of PCNA and Bcl-2, antiapoptotic gene, were markedly decreased in the IT Pa-PDT-treated group compared to the control group. In addition, the levels of cleaved caspase 3, the activated form of caspase 3, and PARP cleavage, a known endogenous substrate for caspases, were significantly increased in the IT Pa-PDT-treated group compared to the control group. These results showed that IT Pa-PDT induced apoptotic cell death through the activation of caspase 3, which plays an important role in apoptosis in the in vivo tumor model.

## DISCUSSION

PDT plays a role in the primary treatment of superficial tumors and is an important treatment option for patients who present with recurrent carcinomas or secondary tumors in oral lesions[15]. Although PDT takes advantage of the relative retention of a photosensitizer by cancer cells, effective delivery of a photosensitizer is of great concern. The IV route of photosensitizer administration

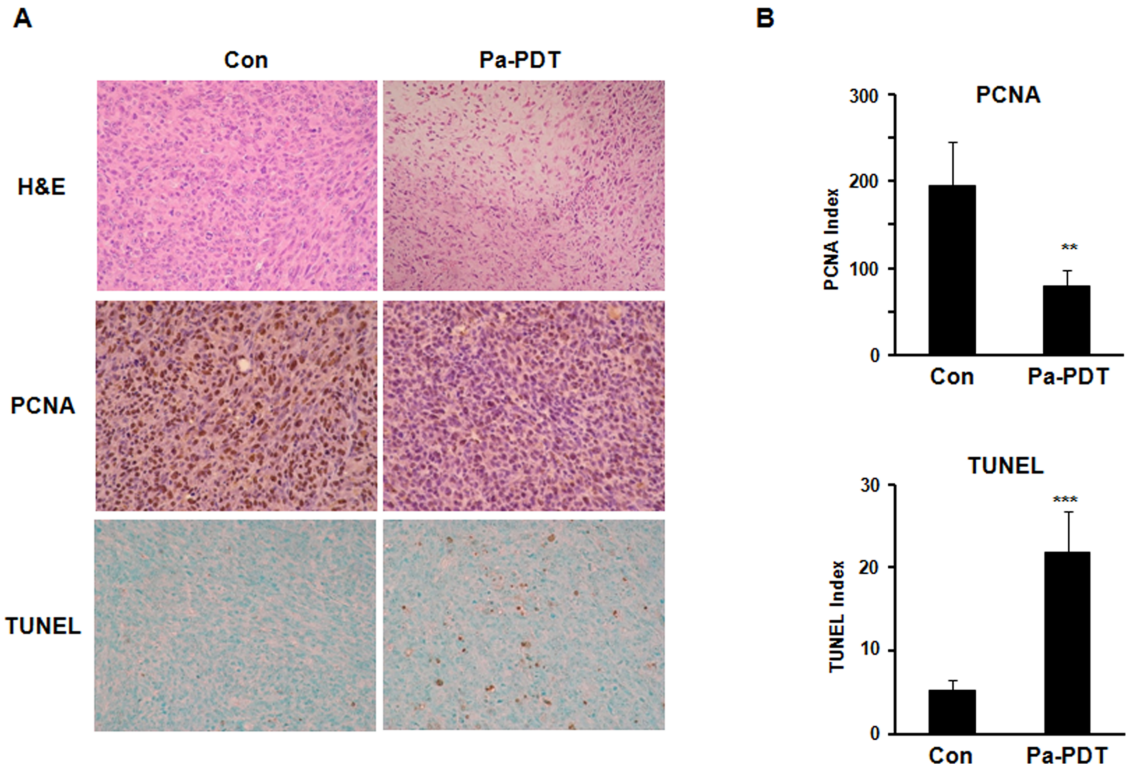


**Figure 5.** Effect of IT Pa-PDT on the proliferation and apoptosis in vivo model. (A) H&E staining of tumor sections (top), immunohistochemistry for PCNA (middle), and TUNEL assay (bottom) were performed on paraffin sections from the tumor. Photographs were taken under a magnification of 200×. (B) Positive cells for PCNA immunostaining (top) and TUNEL (bottom) were counted, and the results are expressed. The data are reported as the mean ± SD of three independent experiments. $^{**}p<0.01$, $^{***}p<0.001$ compared to the control group.

is typically used in clinical and preclinical applications of PDT[21]. However, systemic application of the photosensitizer requires the patient to be isolated from light and have other systemic side effects, such as a hypersensitivity reaction to the photosensitizer compounds[22,23]. Most of the currently used photosensitizer molecules are excited by visible light with limited tissue penetration[24]. Insufficient penetration of the photosensitizer into target tissues can severely limit the outcome of therapy[25]. In addition, the mechanism of tumor-specific accumulation is still not clear[26]. Therefore, several delivery strategies for the photosensitizer have been employed in PDT[27]. Recently, an antitumor reagent has become the appropriate candidate for intratumoral injection against breast, prostate, and bladder tumors and has suppressed the tumor with little toxic side effects[28–30]. The potential advantages for direct intratumoral drug injection include assured precision in the local delivery of drugs, dramatically higher tumor tissue concentrations than is achievable by conventional systemic chemotherapy, complete perfusion of the drug within and around the lesion, and little or no systemic toxic side effects[31]. Referring to these studies, we therefore assumed that intratumoral injection of the photosensitizer may also be an effective delivery strategy for chemotherapy in PDT.

Previously, our study reported the effect of synthesized Pa-PDT on the tumor growth inhibition of oral cancer cells in vitro. High accumulation of synthesized Pa was observed in YD-10B human oral cancer cells, and markedly reduced cell proliferation was confirmed in Pa-PDT-treated YD-10B (human) and AT-84 (murine) oral cancer cells[13,32]. In the present study, we evaluated the in vivo effect of intratumoral injection of synthesized Pa on suppressing tumor growth of murine OSCC AT-84 cells. We determined that once Pa was given intratumorally in a mouse tumor model, successful penetration of Pa was observed by IVIS Imaging System for up to 6 h. Fluorescence imaging has become an important diagnostic tool that is able to detect cancer at an early stage of tumor development and to guide the biopsy of representative samples[33]. Fluorescence can be enhanced by the use of exogenous markers such as photosensitizing drugs. The intensity of the fluorescence by Pa was continuously observed for 14 days, the end of the study period, after IT Pa-PDT using IVIS Imaging System and was still strong in the tumor tissues. These results

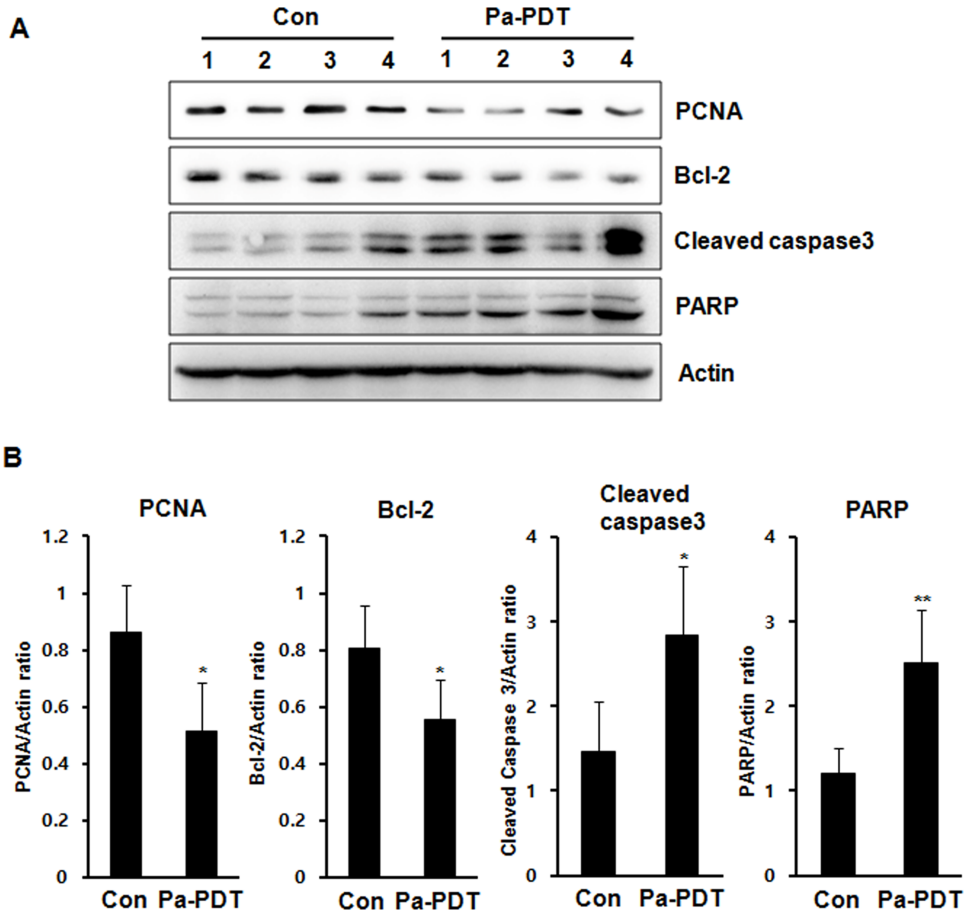


**Figure 6.** The expression of the apoptosis-related protein levels in the tumor tissues. (A) The protein fraction from tumor tissues and the expression levels of PCNA, Bcl-2, cleaved caspase 3, PARP, and actin were detected using Western blot analysis. The protein levels were normalized by a comparison to the actin levels. (B) The bar graft data are reported as the mean ± SD of three independent experiments. *$p < 0.05$, **$p < 0.01$ compared to the control group.

suggested that only a single application of Pa-PDT can effectively induce the inhibition of a solid tumor in vivo and indicated the progression of the tumor using imaging system simultaneously.

PDT light was performed using a laser diode after 2 h. As a result, Pa-PDT by intratumoral administration of Pa significantly decreased the tumor volume compared to the control group. In our previous study, the in vivo effects of IV and intraperitoneal (IP) administration of synthesized Pa were evaluated in the murine oral cancer cell model[32]. We concluded that the IV administration of Pa more effectively inhibited tumor growth than the IP administration of Pa. The effect of tumor growth inhibition by IT Pa-PDT was similar to the IV administration of Pa in the in vivo model. In addition, IT Pa-PDT (2 h) has a short time interval between photosensitizer administration and PDT light treatment compared to IV Pa-PDT (24 h). This result supports the theory that IT Pa-PDT is also an optimal route for the administration of Pa in in vivo assay systems.

Our previous in vitro study identified that synthesized Pa-PDT induced mitochondrial-dependent apoptotic cell death in murine oral squamous cell carcinoma[32]. In the present study, we confirmed the molecular mechanism of cell death by IT Pa-PDT in the in vivo tumor model. Treatment with IT Pa-PDT decreased tumor cell proliferation, as assessed by the immunohistological detection of the proliferation marker PCNA. We also performed TUNEL staining to assess the amount of apoptotic cells in vivo. TUNEL-positive apoptotic cells significantly increased in the cells treated with IT Pa-PDT, compared with the control group. To confirm the apoptotic mechanism of IT Pa-PDT in vivo, we examined the expression levels of apoptosis-related proteins by Western blot. PCNA is widely used as a biomarker for the proliferation in both experimental and clinical pathology, and Bcl-2 is a well-known inhibitor of apoptosis[34–37]. In our study, the levels of PCNA and Bcl-2 expression were markedly decreased, whereas caspase 3 and PARP cleavage activation was increased in IT Pa-PDT-treated tissues.

In conclusion, these results show that IT Pa-PDT effectively arrests tumor growth by inhibiting cell proliferation and inducing apoptosis. Therefore, these findings suggest that IT Pa-PDT could be a potent clinical therapeutic strategy for OSCC. We also predict detection of Pa using the FS system or molecular imaging system, which might improve new approaches for effective simultaneous diagnosis and treatment of OSCC.

*ACKNOWLEDGMENTS: This study was supported by the Basic Science Research Program through the National Research Foundation of Korea (NRF) and funded by the Ministry of Education, Science and Technology (NRF-2014R1A1A2009007, NRF-2016R1D1A1B01006388).*

## REFERENCES

1. Marmur ES, Schmults CD, Goldberg J. A review of laser and photodynamic therapy for the treatment of nonmelanoma skin cancer. Dermatol Surg. 2004;30:264–71.
2. Weishaupt KR, Gomer CJ, Dougherty TJ. Identification of singlet oxygen as the cytotoxic agent in photoinactivation of a murine tumor. Cancer Res. 1976;36:2326–9.
3. Moan J, Berg K. Photochemotherapy of cancer: Experimental research. Photochem Photobiol. 1992;55:931–48.
4. Chiu SM, Oleinick NL. Dissociation of mitochondrial depolarization from cytochrome c release during apoptosis induced by photodynamic therapy. Br J Cancer 2001;84:1099–1106.
5. Karakullukcu B, Nyst HJ, van Veen RL, Hoebers FJ, Hamming-Vrieze O, Witjes MJ, de Visscher SA, Burlage FR, Levendag PC, Sterenborg HJ, Tan IB. mTHPC mediated interstitial photodynamic therapy of recurrent nonmetastatic base of tongue cancers: Development of a new method. Head Neck 2012;34:1597–1606.
6. Santamaria L, Prino G. List of the photodynamic substances. Res Prog Org Biol Med Chem. 1972;3(Pt 1):XI–XXXV.
7. Luna MC, Ferrario A, Wong S, Fisher AM, Gomer CJ. Photodynamic therapy-mediated oxidative stress as a molecular switch for the temporal expression of genes ligated to the human heat shock promoter. Cancer Res. 2000;60:1637–44.
8. Barthwal R, Srivastava N, Sharma U, Govil G. A 500 MHz proton NMR study of the conformation of adriamycin. J Mol Struct. 1994;327:201–20.
9. Wongsinkongman P, Brossi A, Wang HK, Bastow KF, Lee KH. Antitumor agents. Part 209: Pheophorbide-a derivatives as photo-independent cytotoxic agents. Bioorg Med Chem. 2002;10:583–91.
10. Bui-Xuan NH, Tang PM, Wong CK, Fung KP. Photo-activated pheophorbide-a, an active component of Scutellaria barbata, enhances apoptosis via the suppression of ERK-mediated autophagy in the estrogen receptor-negative human breast adenocarcinoma cells MDA-MB-231. J Ethnopharmacol. 2010;131:95–103.
11. Hoi SW, Wong HM, Chan JY, Yue GGL, Tse GM, Law BK, Fong WP, Fung KP. Photodynamic therapy of pheophorbide a inhibits the proliferation of human breast tumour via both caspase-dependent and -independent apoptotic pathways in in vitro and in vivo models. Phytother Res. 2012;26:734–42.
12. You H, Yoon HE, Yoon JH, Ko H, Kim YC. Synthesis of pheophorbide-a conjugates with anticancer drugs as potential cancer diagnostic and therapeutic agents. Bioorg Med Chem. 2011;19:5383–91.
13. Ahn MY, Yoon HE, Kwon SM, Lee J, Min SK, Kim YC, Ahn SG, Yoon JH. Synthesized Pheophorbide a-mediated photodynamic therapy induced apoptosis and autophagy in human oral squamous carcinoma cells. J Oral Pathol Med. 2013;42:17–25.
14. Mroz P, Yaroslavsky A, Kharkwal GB, Hamblin MR. Cell death pathways in photodynamic therapy of cancer. Cancers 2011;3:2516–39.
15. Mohanty N, Jalaluddin M, Kotina S, Routray S, Ingale Y. Photodynamic therapy: The imminent milieu for treating oral lesions. J Clin Diagn Res. 2013;7:1254–7.
16. Cheng Y, Meyers JD, Broome AM, Kenney ME, Basilion JP, Burda C. Deep penetration of a PDT drug into tumors by noncovalent drug-gold nanoparticle conjugates. J Am Chem Soc. 2011;133:2583–91.
17. Orth K, Russ D, Beck G, Rück A, Beger HG. Photochemotherapy of experimental colonic tumours with intratumorally applied methylene blue. Langenbecks Arch Surg. 1998;383:276–81.
18. Chung IS, Son YI, Ko YJ, Baek CH, Cho JK, Jeong HS. Peritumor injections of purified tumstatin delay tumor growth and lymphatic metastasis in an orthotopic oral squamous cell carcinoma model. Oral Oncol. 2008;44:1118–26.
19. Ryu SY, Choi HY, Chang KS, Kim GH, Choi WJ, Ahn SG, Kim YC, Yoon JH, Lee BH. A fiber-based single-unit dual-mode optical Imaging system: Swept source optical coherence tomography and fluorescence spectroscopy. Optics Communications 2012;285:2478–82.
20. Pang S, Kang MK, Kung S, Yu D, Lee A, Poon B, Chen IS, Lindemann B, Park NH. Anticancer effect of a lentiviral vector capable of expressing HIV-1 Vpr. Clin Cancer Res. 2001;7:3567–73.
21. Foster TH, Giesselman BR, Hu R, Kenney ME, Mitra S. Intratumor administration of the photosensitizer pc 4 affords photodynamic therapy efficacy and selectivity at short drug-light intervals. Transl Oncol. 2010;3:135–41.
22. Barcessat AR, Huang I, Rosin FP, dos Santos Pinto D Jr, Maria Zezell D, Corrêa L. Effect of topical 5-ALA mediated photodynamic therapy on proliferation index of keratinocytes in 4-NQO-induced potentially malignant oral lesions. J Photochem Photobiol B 2013;126:33–41.
23. Bredell MG, Besic E, Maake C, Walt H. The application and challenges of clinical PD-PDT in the head and neck region: A short review. J Photochem Photobiol B 2010;101:185–90.
24. Li Z, Wang C, Cheng L, Gong H, Yin S, Gong Q, Li Y, Liu Z. PEG-functionalized iron oxide nanoclusters loaded with chlorin e6 for targeted, NIR light induced, photodynamic therapy. Biomaterials 2013;34:9160–70.
25. Celli JP, Spring BQ, Rizvi I, Evans CL, Samkoe KS, Verma S, Pogue BW, Hasan T. Imaging and photodynamic therapy: Mechanisms, monitoring, and optimization. Chem Rev. 2010;110:2795–838.
26. Takada T, Tamura M, Yamamoto T, Matsui H, Matsumura A. Selective accumulation of hematoporphyrin derivative in glioma through proton-coupled folate transporter SLC46A1. J Clin Biochem Nutr. 2014;54:26–30.
27. Park S. Delivery of photosensitizers for photodynamic therapy. Korean J Gastroenterol. 2007;49:300–13.
28. Shikanov A, Shikanov S, Vaisman B, Golenser J, Domb AJ. Paclitaxel tumor biodistribution and efficacy after intratumoral injection of a biodegradable extended release implant. Int J Pharm. 2008;358:114–20.

29. Al-Ghananeem AM, Malkawi AH, Muammer YM, Balko JM, Black EP, Mourad W, Romond E. Intratumoral delivery of paclitaxel in solid tumor from biodegradable hyaluronan nanoparticle formulations. AAPS PharmSciTech 2009; 10:410–7.
30. Shikanov S, Shikanov A, Gofrit O, Nyska A, Corn B, Domb AJ. Intratumoral delivery of paclitaxel for treatment of orthotopic prostate cancer. J Pharm Sci. 2009;98:1005–14.
31. Celikoglu F, Celikoglu SI, Goldberg EP. Bronchoscopic intratumoral chemotherapy of lung cancer. Lung Cancer 2008;61:1–12.
32. Ahn MY, Kwon SM, Kim YC, Ahn SG, Yoon JH. Pheophorbide a-mediated photodynamic therapy induces apoptotic cell death in murine oral squamous cell carcinoma in vitro and in vivo. Oncol Rep. 2012;27:1772–8.
33. Guyon L, Ascencio M, Collinet P, Mordon S. Photodiagnosis and photodynamic therapy of peritoneal metastasis of ovarian cancer. Photodiagnosis Photodyn Ther. 2012;9:16–31.
34. van Diest PJ, Brugal G, Baak JP. Proliferation markers in tumours: Interpretation and clinical value. J Clin Pathol. 1998;51:716–24.
35. Celis JE, Celis A. Cell cycle-dependent variations in the distribution of the nuclear protein cyclin proliferating cell nuclear antigen in cultured cells: Subdivision of S phase. Proc Natl Acad Sci USA 1985;82:3262–6.
36. Kurki P, Vanderlaan M, Dolbeare F, Gray J, Tan EM. Expression of proliferating cell nuclear antigen (PCNA)/cyclin during the cell cycle. Exp Cell Res. 1986;166:209–19.
37. Wang HG, Reed JC. Mechanisms of Bcl-2 protein function. Histol Histopathol. 1998;13:521–30.